Kinetic and Secondary Structure Analysis of *Naegleria andersoni* GIR1, a Group I Ribozyme Whose Putative Biological Function Is Site-Specific Hydrolysis†

Evelyn Jabri, Stefan Aigner, and Thomas R. Cech*

Department of Chemistry and Biochemistry, Howard Hughes Medical Institute, University of Colorado, Boulder, Colorado 80309-0215

Received July 30, 1997; Revised Manuscript Received October 15, 1997⊗

ABSTRACT: NanGIR1 is a catalytic element inserted in the P6 loop of a group I intron (NanGIR2) in the small subunit rRNA precursor of the protist *Naegleria andersoni* [Einvik, C., Decatur, W. A., Embley, T. M., Vogt, V. M., and Johansen, S. (1997) *RNA 3*, 710−720]. It catalyzes site-specific hydrolysis at an internal processing site (IPS) after a G residue that immediately follows the P9 stem−loop. Functional and structural analyses were initiated to compare NanGIR1 to group I introns that carry out self-splicing. Chemical modification and site-directed mutagenesis studies showed that NanGIR1 shares many structural elements with other group I introns, but also contains a pseudoknot (P15), which is important for catalytic activity. Deletion analysis revealed the boundaries of the minimum self-cleaving unit (178 nucleotides). The rate of self-cleavage was measured as a function of mono- and divalent ion concentration, temperature, and pH. The reaction at the IPS yields 5′-phosphate and 3′-hydroxyl termini, requires Mg^{2+}or Mn^{2+} ions, and is first-order in [OH^-] between pH 5.0 and 8.5. The latter results suggest that the nucleophile in the reaction is hydroxide or possibly a Mg^{2+}-coordinated hydroxide. With a second-order rate constant of 1×10^5 min^{-1} M^{-1}, the self-cleavage reaction of NanGIR1 is 2 orders of magnitude faster than a similar site-specific hydrolysis reaction of the circular form of the *Tetrahymena* group I intron.

Group I introns interrupt the genes of ribosomal RNAs (rRNA), transfer RNAs (tRNA), and messenger RNAs (mRNA) in a variety of organisms (*1*−*3*). The intron RNAs fold into well-defined secondary and tertiary structures consisting of paired segments, designated P1−P10, as well as single-stranded joining segments (J) and hairpin loops (L) (Figure 1A). The catalytic core, important for splicing, is composed of P3−P8 (for review, see ref 4). *In vitro*, many group I intron RNAs are capable of self-splicing in the absence of a protein component. *In vivo*, splicing of some group I introns is assisted by proteins (*5*). In the presence of guanosine, these introns excise themselves from the surrounding exon sequences in a two-step transesterification reaction. In the first step, the 5′-splice site (5′SS)[1] is cleaved as an exogenous molecule of guanosine is added to the 5′-end of the intron. In the second step, the 3′-splice site (3′SS) is cleaved concomitantly with exon ligation (*4*). The 3′-terminal G, which binds in the G-binding site in helix P7 for the second step of splicing (*6*, *7*), is positioned by interactions involving P9, P9.0, and P10.

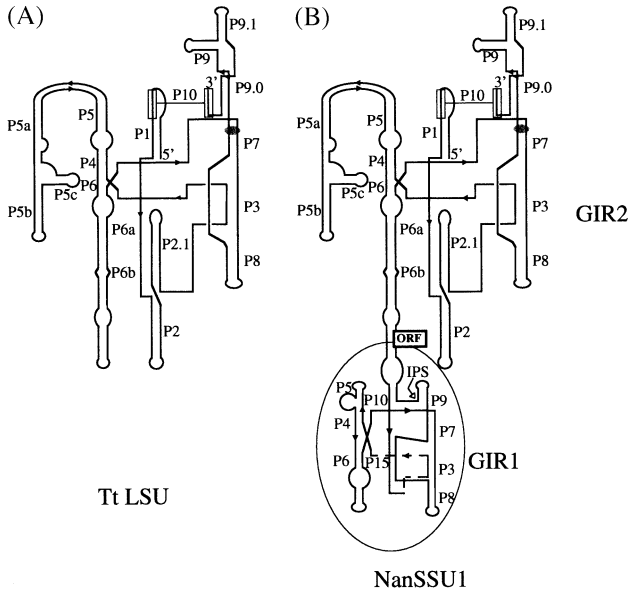

FIGURE 1: Schematic comparison of two group I introns. Secondary structure model for (A) *Tetrahymena* TtLSU intron (*57*) and (B) NanSSU1 intron. GIR1 catalyzes site-specific hydrolysis at the internal processing site (IPS). GIR2 is a typical self-splicing group I intron (*17*). Gray oval shows the position of the G-binding site. ORF means that an open reading frame was inserted at this location.

Although best known for their self-splicing ability, group I introns and ribozymes engineered from them can catalyze other reactions such as site-specific cleavage or ligation of oligonucleotides (*8*−*10*), circularization of excised introns (*11*, *12*), and hydrolysis at the 3′SS (*4*, *11*). The 3′SS hydrolysis reaction, considered a side reaction for group I introns, leaves a 5′-phosphate and a 3′-hydroxyl group at the newly created termini. The reaction depends on both

† This work was supported in part by NIH Postdoctoral Grant GM18123 to E.J. and a Deutscher Akademischer Austauschdienst grant to S.A. S.A. is a Regensburg fellow. T.R.C. is an investigator of the Howard Hughes Medical Institute and an American Cancer Society Professor.

* To whom correspondence should be addressed: Department of Chemistry and Biochemistry, Campus Box 215, University of Colorado, Boulder, CO 80309-0215. E-mail: thomas.cech@colorado.edu.

⊗ Abstract published in *Advance ACS Abstracts,* November 15, 1997.

[1] Abbreviations: Dir, *Didymiun iridis*; Nan, *Naegleria andersoni*; GIR1, group I ribozyme 1; ORF, open reading frame; SS, splice site; IPS, internal processing site; DMS, dimethyl sulfate; CMCT, *N*-cyclohexyl-*N*′-[2-(*N*-methyl-4-morpholino)ethyl]carbodiimide *p*-toluenesulfonate; eu, calories per mole per kelvin.

S0006-2960(97)01859-X CCC: $14.00

an active conformation of the catalytic core and recognition of the conserved G at the 3′-end of the intron (*13*, *14*), but not on the presence of an internal guide sequence (IGS) (*15*).

This site-specific hydrolysis reaction takes on biological significance because six naturally occurring introns, with predicted group I-like secondary structure, have 3′SS hydrolysis as their presumptive function (*16*, *17*). Johansen and Vogt (*18*) reported that DiSSU1, a mobile intron in the nuclear rRNA gene of *Didymium iridis*, contains two distinct catalytic centers, GIR1 and GIR2. *In vitro*, GIR1 catalyzes site-specific hydrolysis at two internal processing sites (IPS1 and IPS2), while GIR2 catalyzes the typical group I splicing reactions. Decatur and colleagues (*16*) hypothesized that GIR1 functions in the processing of the mRNA for I-*Dir*I, the homing endonuclease encoded by the open reading frame (ORF) embedded within the DiSSU1 intron.

Phylogenetic sequence comparison and site-directed mutagenesis resulted in a preliminary secondary structure model for *D. iridis* GIR1 (*16*). DirGIR1 IPS1 resembles a 3′SS as defined for other group I introns, in that it is flanked on the 5′-side by a conserved guanosine residue. A novel 6 bp P15 pseudoknot was proposed, and mutational analysis established that it is important for catalysis (S. Johansen, personal communication). In contrast to GIR2, the downstream group I intron involved in a more typical self-splicing reaction, GIR1 lacks a P1 element (containing the IGS sequence) and the conserved A residues in J4/5 (required for G addition and exon ligation).

Recently, GIR1 introns were identified in five species of the protist *Naegleria* (*17*). They are all embedded within loop 6 of a self-splicing GIR2 intron and are always associated with an ORF (Figure 1B) encoding a protein with sequence hallmarks of a distinct family of homing endonucleases (*19*). Comparative sequence analysis predicts that GIR1s from *Naegleria* (NaGIR1) have group I-related structures (Figure 1B) much like that of DirGIR1 (*16*), and probably function in maturation of the intronic mRNA (*17*).

Here, we provide the first kinetic and mechanistic analysis of this novel catalytic element. We also determine the approximate boundaries of the active unit of GIR1 from *Naegleria andersoni* (NanGIR1), examine its metal ion cofactor requirements, and probe its secondary structure through chemical modification and site-directed mutagenesis. Since all GIR1 RNAs appear to have similar secondary structures and functions, the results of this study should be generally applicable to other members of this new family of group I introns.

MATERIALS AND METHODS

Plasmid Construction. DNA primers were synthesized on an Applied Biosystems 380B DNA synthesizer. PCR was done in 100 μL reaction mixtures containing 10 mM Tris-HCl (pH 8.3), 4 mM $MgCl_2$, 50 mM KCl, each dNTP at 0.2 mM, and 2.5 units of *Taq* polymerase, using DNA from the genomic plasmid pNanG1-290 (a gift from S. Johansen). The 5′-primers encoded a *Bam*HI restriction endonuclease site for cloning, a promoter for T7 RNA polymerase, and sequences corresponding to various 5′-regions of GIR1. Each 3′-primer encoded one of three different sequences complementary to the 3′-end of NanGIR1, an *Ear*I site to permit termination of T7 RNA polymerase transcription, and an *Eco*RI site for cloning. The DNA was denatured for 4 min at 94 °C and then amplified in 30 cycles for 1 min at 94 °C, 1 min at 55 °C, and 2 min at 72 °C. The resulting DNA was purified from a 4% NuSieve (FMC Corp.) agarose gel using a Qiagen gel extraction kit. Oligodeoxynucleotides containing appropriate changes were used in a similar procedure to introduce mutations within the molecule. The DNA was subsequently digested with *Bam*HI and *Eco*RI, ligated into a pUC19 plasmid, and used to transform competent XL1-Blue cells using a Bio-Rad gene pulser (1.8 kV, 400 Ω). Clones were screened using restriction endonuclease digestion and verified by sequencing (U.S. Biochemicals Sequenase kits).

Transcription Reaction. For preparation of uniformly labeled RNA, 20 μL reaction mixtures contained 40 mM Tris-HCl (pH 7.5), 15 mM $MgCl_2$, 10 mM DTT, 2 mM spermine, each NTP at 1 mM, ~1 μg of DNA template digested with *Ear*I, 50 μCi of [α-^{32}P]ATP, and T7 RNA polymerase and were incubated at 25 °C for 2 h. The RNA transcripts were purified on an 8% polyacrylamide gel. All gels contained 29:1 acrylamide/bis, 8 M urea, and 1× TBE (1× TBE is 0.1 M Tris base, 0.083 M boric acid, and 1 mM EDTA). Gel slices containing the labeled RNA were crushed and then soaked in TE [10 mM Tris-HCl (pH 7.5) and 1 mM EDTA] at 4 °C overnight. Acrylamide was removed by filtration, and the solution was subsequently ethanol precipitated. Purified RNA was dissolved in a small volume (20−50 μL) of distilled, deionized water.

Self-Cleavage Reaction. RNA was preincubated at 45 °C for various lengths of time in 10 mM potassium cacodylate buffer (pH 5.5), 25 mM $MgCl_2$, and various concentrations of KCl, unless otherwise noted. The site-specific hydrolysis reaction was initiated with a pH jump by addition of 4 volumes of 47.5 mM K-HEPES (pH 7.5) containing the same concentrations of $MgCl_2$ and KCl as in the preincubation. Aliquots (2.5 μL) were removed at various intervals, and the reaction was quenched with the addition of 2 volumes of ice cold stop solution containing 94% formamide, 0.1× TBE, 50 mM EDTA, 0.025% xylene cyanol, and 0.025% bromophenol blue. Samples were analyzed on 8% polyacrylamide/urea gels. The gels were imaged and quantitated using ImageQuant 3.0 Software and a Molecular Dynamics PhosphorImager.

Data Analysis. Kinetic data were first plotted as the fraction precursor remaining versus time (for an example, see Figure 4B). The fraction of precursor remaining was calculated as precursor/(precursor + product 1), where product 1 was the large hydrolysis product (i.e. 5′ to the IPS). Values were not corrected for the loss of the small hydrolysis product, product 2, which was routinely run off of the gel to facilitate quantitation of the other bands. The curves were fit to standard nonlinear first-order decay equations with an end point correction, $(\text{fraction of precursor})_t = (\text{fraction of precursor})_{t=\infty} + (\text{fraction of precursor})_{t=0} \times \exp(-k_{obs}t)$, to obtain the rate constant, k_{obs}. Subsequent analyses of k_{obs} versus various factors as well as analyses of other kinetic parameters were completed using Kaleidagraph v 3.0 (Abelbeck Software).

Determining the Position of the Internal Processing Site (IPS). The position of the IPS was determined using the method of Zaug and colleagues (*20*) with minor modifications. Product 1, the 178-nucleotide RNA corresponding to the sequence 5′ of the IPS (intron sequence), was generated by preincubating precursor in standard hydrolysis reaction

mixtures and passing the reaction mixture over a G-25 spin column to remove the KCl and stop the reaction. Subsequent addition of the poly(A) tail, RT-PCR, and sequencing were done as reported earlier (*20*).

Product 2, the 19-nucleotide RNA 3′ to the IPS (exon sequence), was isolated from standard self-cleavage reaction by gel purification. The 5′-phosphate was removed by incubating 20 pmol of RNA with 1 unit of calf intestinal phosphatase in 15 mM Tris (pH 8.0) at 37 °C for 1 h. The RNA was phenol/chloroform extracted, ethanol precipitated, and resuspended in H_2O. The sample (8 mL final volume) was heated at 95 °C for 3 min in the presence of 10× polynucleotide kinase (PNK) buffer (NEB) and then iced. After the mixture was cooled to 37 °C, 1 unit of PNK and 1 μL of [γ-^{32}P]ATP were added to the reaction (10 μL final volume), and the sample was incubated at 37 °C for 30 min. The 5′-end-labeled RNA was gel purified as described above. Product 2 was sequenced by limited treatment with sequence-specific ribonucleases (*21*).

Chemical Modification. For each reagent, 10 μg (150 pmol) of refolded pre-NanGIR1 RNA (197 nucleotides), in a 200 μL final sample volume, was modified at 25 °C in buffer containing 25 mM $MgCl_2$ and 1 M KCl. DMS (Aldrich) treatment was done in HKM buffer [80 mM K-HEPES (pH 7.0), 800 mM KCl, and 25 mM $MgCl_2$] in the presence of 2 μL of diluted DMS (2 μL of DMS diluted with 5 μL of ethanol) for 30 min and stopped by addition of 100 μL of a solution containing 0.5 M β-mercaptoethanol and 0.75 M NaOAc (pH 5.5). CMCT (Sigma) treatment was done in BKM buffer [80 mM potassium borate (pH 8.1), 800 mM KCl, and 25 mM $MgCl_2$] in the presence of 20 μL of CMCT stock (42 mg/mL in BKM buffer) for 30 min, and 250 μL of 0.5 M potassium borate (pH 6.1) was added prior to precipitation. Kethoxal (U.S. Biochemicals) treatment was done in HKM buffer in the presence of 20 μL of kethoxal (37 mg/mL in 20% ethanol) for 60 min, and 10 μL of 0.5 M potassium borate (pH 7.0) was added prior to precipitation. For each reaction, a control was treated in parallel, omitting the chemical reagent. All samples were precipitated with 3 volumes of ethanol on dry ice immediately following modification. The RNA pellet was resuspended in 500 μL of TE at pH 7.0 (for DMS- and CMCT-modified samples) or 25 mM potassium borate at pH 7.0 (for kethoxal-modified samples), desalted, and concentrated by dialysis through a Microcon-30 microconcentrator (Amicon).

Primer Extension. Primer extension was performed essentially as described by Zaug and Cech (*22*) using DNA primers Nan195−177, corresponding to residues 197−177, and Nan125−111, corresponding to residues 125−111 of NanGIR1. 5′-End-labeled primer (1 pmol, ∼1.5 × 10^6 cpm/pmol) was annealed to approximately 0.5 pmol of modified or control RNA in 6 μL of AB buffer [50 mM Tris-HCl (pH 8.3), 60 mM NaCl, and 10 mM DTT] by boiling for 1 min and then cooling to room temperature. Reverse transcription was carried out with 1 unit of AMV reverse transcriptase (Life Sciences) in 15 μL of RT buffer [50 mM Tris-HCl (pH 8.3), 6 mM $Mg(OAc)_2$, 60 mM NaCl, and 10 mM DTT] in the presence of each dNTP at 0.4 mM at 25 °C for 30 min. Transcription was stopped by addition of an equal volume of formamide stop solution. Transcripts were resolved on 12% polyacrylamide/urea gels and analyzed as described above.

For each reagent, the modification lanes and the respective control lanes were scanned and normalized to the same total number of counts per lane. The counts in the control lanes were then subtracted from those in the modification lane. For each reagent and each of the four nucleotides, the strongest modification was set as 100%, except for the DMS modification of A51 and the CMCT modification of U99, since these nucleotides proved to be hyperactive (see Figure 6). In these two cases, the second-strongest hits were used as references. Reactivities were assigned as follows: 0−20%, no reactivity; 20−40%, weak reactivity; and >40%, strong reactivity. These criteria were chosen because they agreed with visual assessment of the band intensities and took into account the different reactivities of the four bases with respect to modification by the reagents.

Preliminary chemical modification trials at 45 °C were carried out to examine the effect of the reaction conditions on the RNA. Uniformly labeled pre-NanGIR1 was treated as described and analyzed by gel electrophoresis. Quantitation of the RNA bands showed that the population of self-cleavage products formed during the reactions varied for the different modification reagents with 5, 71, and 5% of product 1 being formed for DMS, CMCT, and kethoxal, respectively. Since self-cleavage during modification leads to a mixture of RNAs and could potentially complicate data interpretation, modification was done at 25 °C, a temperature at which essentially no RNA self-cleavage is observed (data not shown). To quantitate the degree of self-cleavage during incubation with the reagents at 25 °C, uniformly labeled pre-NanGIR1 was treated the same way as it was in the modification experiments and subsequently analyzed by denaturing polyacrylamide gel electrophoresis. PhosphorImager quantitation of the bands showed that the population of full length precursor comprised 98% after refolding, and 97, 93, and 94% of the total RNA after DMS, CMCT, and kethoxal modifications, respectively (data not shown).

RESULTS

Minimal Functional Pre-NanGIR1. Deletion analysis was used to identify the boundaries of the intron. Nine different plasmids (Figure 2A) were constructed to generate pre-NanGIR1 RNAs with 161, 169, 175, 178, 182, 189, and 199 nucleotides upstream and 10, 12, or 19 nucleotides downstream of the IPS (demonstration of the occurrence of a single internal processing site is described below). To maximize transcription by T7 RNA polymerase, all clones were modified to begin transcription with three guanosines followed by the pre-NanGIR1 sequence. After RNA transcription, the unprocessed RNA was gel purified and incubated under conditions favoring self-cleavage. The construct with 178 nucleotides preceding and 19 nucleotides following the IPS (pre-NanGIR1−197) was the most efficient at site-specific hydrolysis (Figure 2A). All constructs carried out hydrolysis at the IPS except that with 161 nucleotides upstream and 10 nucleotides downstream of the IPS, which was inactive. Catalytic activity of the inactive construct could be restored, albeit at a very slow rate, by extending the region downstream of the IPS from 10 to 12 nucleotides (data not shown). These results indicate that NanGIR1 intron is ∼178 nucleotides long and requires more than 12 nucleotides downstream of the IPS for maximum cleavage. Construct pre-NanGIR1−197 was used in the subsequent determination of optimal conditions for hydrolysis. The

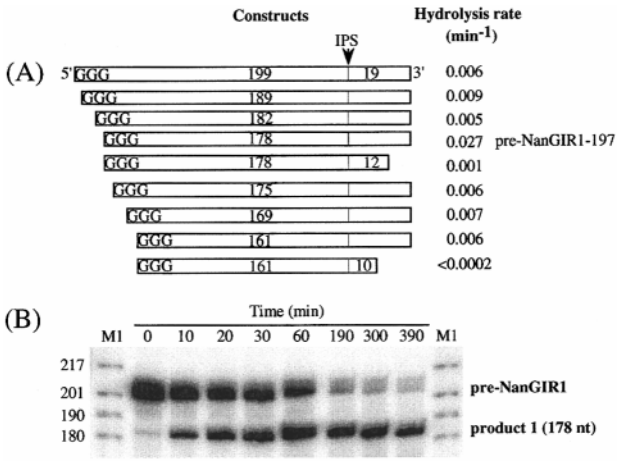

FIGURE 2: Deletion analysis carried out to identify the minimal active sequence for pre-NanGIR1. (A) For this experiment, gel-purified RNA from each construct was mixed with the reaction buffer [40 mM Tris-HCl (pH 7.5), 25 mM $MgCl_2$, 1 M KCl, 2 mM spermidine, and 1 mM DTT], and hydrolysis was initiated by incubating the reaction mixture at 45 °C. Self-cleavage of pre-NanGIR1 at the IPS (arrow and line) produced product 1 (nucleotides 5′ to the IPS) and product 2 (nucleotides 3′ to the IPS). Numbers in the box indicate the number of nucleotides either 5′ or 3′ to the IPS. The three guanosine residues at the 5′-end of the constructs are not native sequence but a result of introducing a T7 RNA polymerase promoter. (B) A representative gel of the hydrolysis of uniformly ^{32}P-labeled pre-NanGIR1−197 used to produce product 1 (178 nucleotides) and product 2 (19 nucleotides, routinely run off the gel to facilitate quantitation of precursor and product 1 bands). The decrease in the total radioactivity with increasing time is due to the nonspecific cleavage of pre-NanGIR1 during the long incubation times. M1 represents ^{32}P-end-labeled pBR322 *Msp*I DNA markers.

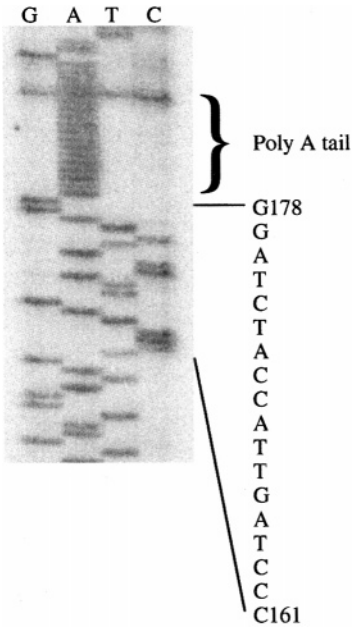

FIGURE 3: Cleavage site determination. Product 1 RNA was poly-(A) tailed using the method of Zaug and colleagues (*20*). cDNA was synthesized using reverse transcriptase with a primer ending in 18 T residues and an *Eco*RI restriction site (EcodT18). PCR with the EcodT18 primer and a primer with a *Bam*HI restriction site, T7 promoter, and the sequence corresponding to nucleotides 19−36 of NanGIR1 produced a 210-nucleotide fragment of DNA. The PCR product was cloned into pUC19 as described in Materials and Methods, and multiple clones were sequenced using dideoxynucleotides; a representative example is shown here. The results showed that the site of cleavage follows G178.

RNA resulting from transcription of pre-NanGIR1−197 will hereafter be referred to as pre-NanGIR1.

Determination of the Cleavage Site. The hydrolysis reaction gave products of ~180 nucleotides (Figure 2B) and ~20 nucleotides (not shown). To determine the exact site of hydrolysis, the 3′-end of product 1 was sequenced as previously described (*20*). This RNA was tailed using ATP and yeast poly(A) polymerase without any additional treatment, thereby establishing that it had a 3′-OH. Following PCR amplification and cloning of the cDNA, dideoxy sequencing of product 1 showed that the cleavage site was located 178 nucleotides from the 5′-end of pre-NanGIR1 following G178 (Figure 3). 5′-End labeling of product 2 with [γ-^{32}P] ATP and PNK was successful only when the RNA was first treated with phosphatase, indicating the presence of a 5′-phosphate group. Limited RNase digestion of product 2 showed that it was 19 nucleotides long with a sequence corresponding to the 3′-end of the pre-NanGIR1 transcript (data not shown). These results indicate that hydrolysis of pre-NanGIR1 *in vitro* occurs after G178 and generates 5′-phosphate and 3′-hydroxyl termini. L-Arginine amide, an inhibitor which blocks the binding of guanosine at the G-binding site of other group I introns (K_i of 0.7 mM for the *Tetrahymena* intron) (*23*), also inhibits hydrolysis at G178 (at ≥1 mM; data not shown).

Although it has been reported that pre-NanGIR1 undergoes cleavage at this same IPS as well as at a second site within product 2 (*17*), we did not see any indication of this second reaction. This difference most probably stems from the differences in the size of the constructs used; our pre-NanGIR1 construct is ~90 nucleotides shorter at the 5′-end and ~30 nucleotides shorter at the 3′-end than that of Johansen and colleagues (*17*). We did detect an additional cleavage site within product 1 in the absence of a competent IPS, which appeared after approximately 4 h of reaction (data not shown).

Determination of the Optimal Reaction Conditions. Initial reactions with pre-NanGIR1 were carried out under the same conditions reported for pre-DirGIR1 [40 mM Tris-HCl (pH 7.5), 25 mM $MgCl_2$, 1 M KCl, 2 mM spermidine, and 5 mM DTT at 45 °C] (*16*). When purified pre-NanGIR1 was incubated under these conditions for 6 h, ~95% cleavage was observed (Figure 2B) with a rate constant (k_{obs}) of 0.030 ± 0.003 min^{-1}.

Without prior folding of the RNA, a 30 min lag phase preceded the reaction. Standard renaturation protocols (*24*, *25*) failed to alleviate this problem. Preincubation in a solution more closely resembling the cleavage buffer [10 mM potassium cacodylate (pH 5.5), 25 mM $MgCl_2$, and 1 M KCl for 30 min at 45 °C] followed by initiation of the reaction by a pH jump yielded kinetic traces without a lag phase. No significant hydrolysis was observed during this preincubation, which was therefore employed in subsequent reactions.

Divalent Cation Requirement. The $MgCl_2$ requirement was examined at several concentrations of KCl. No site-specific hydrolysis was observed in the absence of $MgCl_2$ even in the presence of 1 M KCl. Reactivity increased with increasing concentrations of Mg^{2+}, reaching a maximum at ~25 mM $MgCl_2$ (Figure 4A). Similar Mg^{2+} profiles were observed at various concentrations (250, 500, and 1000 mM) of KCl (data not shown). Metal ion specificity was also tested. $CaCl_2$ did not substitute for $MgCl_2$ and appeared to promote nonspecific hydrolysis (data not shown). $MnCl_2$,

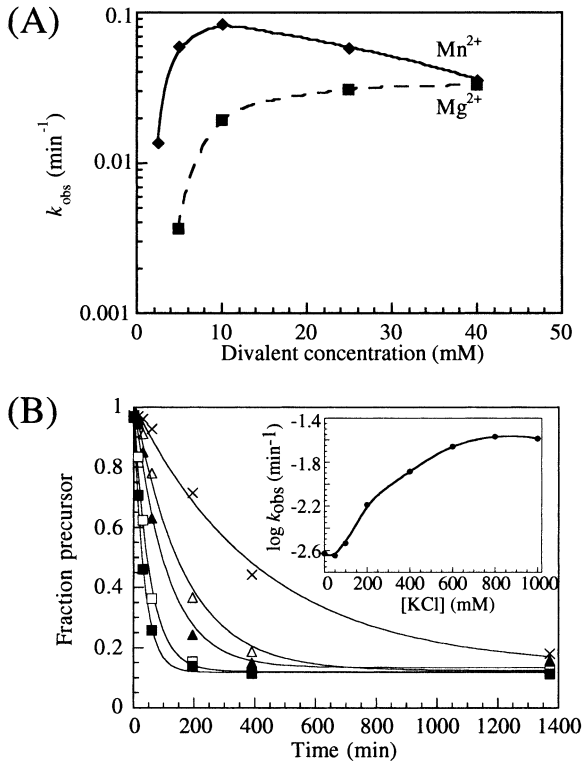

FIGURE 4: Effects of metal ions on the rate of hydrolysis. (A) Variation in k_{obs} as a function of $MgCl_2$ and $MnCl_2$ concentration. Pre-NanGIR1 was refolded as described; the reaction was initiated with a pH jump to 7.5 with the addition of 47.5 mM Tris-HCl (pH 7.5), 1 M KCl, and 0−40 mM $MgCl_2$ or $MnCl_2$, and incubation proceeded at 45 °C for various lengths of time. Each value of k_{obs} is based on analysis of 7−10 time points. No cleavage was observed in the absence of divalent cations. (B) Kinetic analysis of cleavage at IPS as a function of KCl concentration. Plots showing the disappearance of pre-NanGIR1 with time at KCl concentrations of (×) 0 mM, (△) 200 mM, (▲) 400 mM, (□) 600 mM, and (■) 1 M. All data were fit as described in Materials and Methods. The inset shows the increase in the observed rate constant (k_{obs}) as a function of KCl concentration. The line is an interpolation of data points.

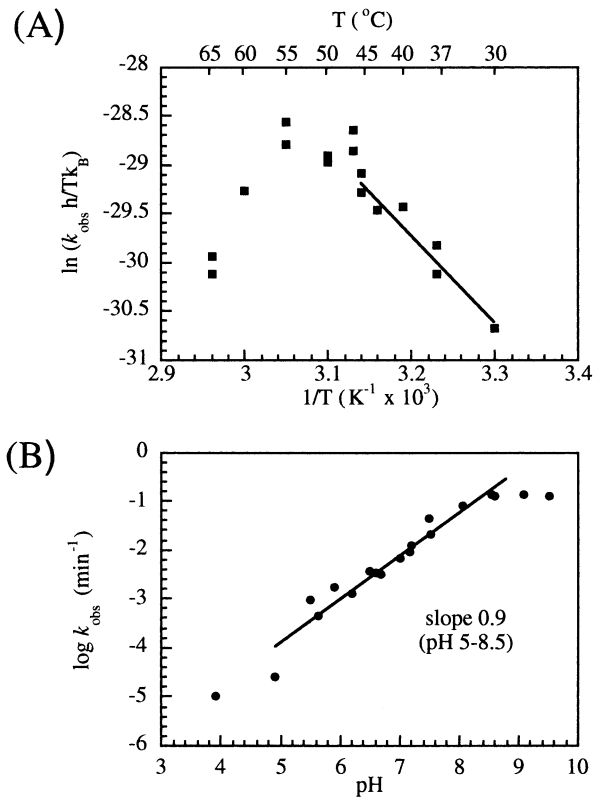

FIGURE 5: Optimization of site-specific cleavage conditions. (A) Eyring plot of k_{obs} as a function of temperature. h is Planck's constant, and k_B is the Boltzman constant. (B) Pre-NanGIR1 was incubated as described except that five different buffers were used to span the pH range examined: 40 mM acetate (pH 4.0−5.5), 40 mM MES (pH 5.5−6.5), 40 mM PIPES (pH 6.0−7.5), 40 mM HEPES (pH 6.5−8.5), and 40 mM CHES (pH 8.5−10.0). Error is associated with the low-pH points due to low reactivity of the RNA at pH <5.0, and with the data at pH >9 due to nonspecific degradation of the RNA, which made it difficult to quantitate product 1.

however, did efficiently replace $MgCl_2$. At lower concentrations (5−20 mM), $MnCl_2$ was more effective than $MgCl_2$ at promoting site-specific hydrolysis, but higher concentrations (>25 mM) resulted in decreased activity.

Monovalent Cation Requirement. Monovalent salts stimulated both folding and reactivity of pre-NanGIR1. For efficient folding, as shown by the absence of the initial lag phase, at least 500 mM KCl was required (data not shown). The rate of site-specific cleavage was stimulated 10-fold in 1 M KCl compared to the reaction in its absence (Figure 4B). Monovalent ion specificity was tested by substituting other salts for KCl. NaCl resulted in an only 5-fold increase in the reaction; ammonium ions had no positive effect, and Li^+ was inhibitory (1 M LiCl resulted in a 15-fold reduction in the hydrolysis rate constant). The reaction of pre-NanGIR1 in the presence of 1 M K^+, Na^+, or NH_4^+ produced the same products as reaction in the absence of added monovalent ions (data not shown).

At low concentrations of monovalent cations, polyamines such as spermine and spermidine bind to the polyanionic RNA and provide structural stabilization (*26*, *27*). We hypothesized that addition of spermine or spermidine could eliminate or reduce the requirement for monovalent cations. However, we found that neither spermine nor spermidine, at concentrations used for other introns (≤4 mM) (*27*), could replace the monovalent ion. Furthermore, addition of either compound to reaction mixtures containing various concentrations of KCl (100−1000 mM) did not affect the rate of hydrolysis (data not shown).

Temperature Dependence. The hydrolysis rate constant was measured between 30 and 65 °C under conditions (25 mM $MgCl_2$ and 1 M KCl) that favor maximal activity at 45 °C. Between 30 and 45 °C, a monotonic increase in activity was observed. An Eyring analysis of these data yielded the following activation parameters: $E_a = 27 \pm 4$ kcal mol^{-1}, $\Delta H^{\ddagger} = 26 \pm 4$ kcal mol^{-1} K^{-1}, and $\Delta S^{\ddagger} = 6 \pm 10$ eu (Figure 5A). The entropy of activation has considerable error, resulting from the limited temperature range available for this analysis, but nevertheless, it is clear that $T\Delta S^{\ddagger}$ is small compared to $\Delta H^{\ddagger}$. Above 47 °C, the hydrolysis rate plateaued and then dropped as the temperature increased. This behavior is consistent with unfolding of the RNA tertiary structure at the elevated temperatures. NanGIR1 has a temperature profile similar to that of the *Anaebena* self-splicing intron, and it is not as thermostable as the *Azoarcus* intron (*28*).

pH Dependence. The effect of hydroxide ion concentration on the rate of self-cleavage was determined over a pH range of 4.5−9.5 (Figure 5B). Use of different buffers at the same pH did not affect the rate of hydrolysis, indicating that the observed pH effects were not buffer-specific. As

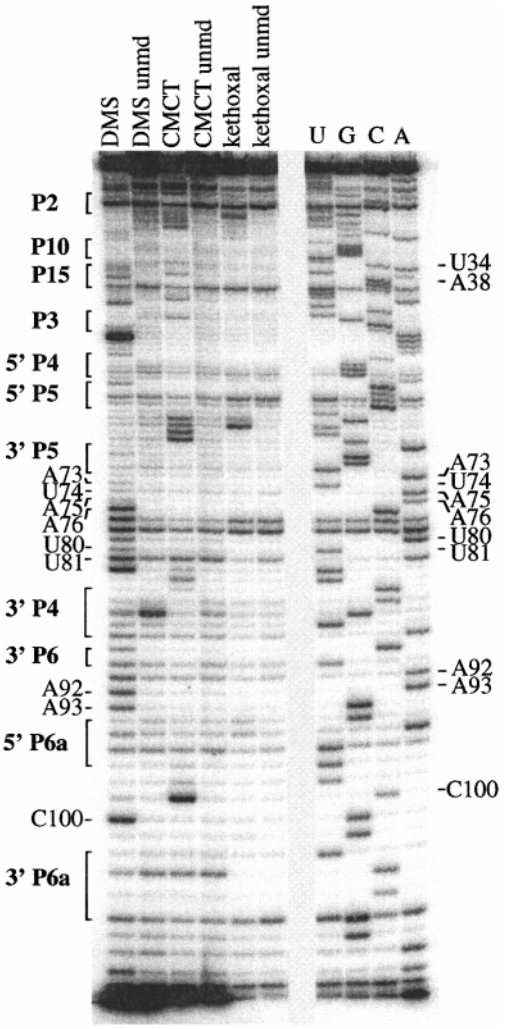

FIGURE 6: Probing the secondary structure using chemical modification. The gel shows the sites of chemical modification of pre-NanGIR1 RNA with DMS, CMCT, and kethoxal revealed by reverse transcription from primer Nan195−177. Reverse transcriptase stops or pauses one nucleotide prior to a modified base, resulting in the modification bands being one nucleotide "ahead" of their corresponding sequencing bands. Control samples that were not exposed to the modifying reagents but otherwise treated equally are included for each reagent (unmd). Lanes U, G, C, and A show dideoxy chain termination sequencing of unmodified pre-NanGIR1.

shown in Figure 5B, the reaction rate is first-order in [OH^-] from pH 4 or 5 to 8.5 and then plateaus.

Probing the Reaction Site Requirements. In analogy to the 3′SS reaction of other group I introns, the G nucleotide preceding the IPS (G178) was expected to be important for reactivity and to bind in the G site in P7. Mutation of G178 to the three other nucleotides resulted in a complete loss of activity (data not shown).

Probing Secondary Structure. To obtain information about the secondary structure of pre-NanGIR1, chemical modification was performed with DMS, CMCT, and kethoxal. Subsequent reverse transcription reveals the modified bases because modifications cause reverse transcriptase (RT) to pause or terminate, resulting in bands preceding these positions by one nucleotide when analyzed by denaturing polyacrylamide gel electrophoresis (*29*, *30*) (Figure 6). The chemical modification pattern of pre-NanGIR1 was determined by extension of two primers that allowed all positions to be evaluated, except for the primer binding site at the 3′-terminus (Figure 7).

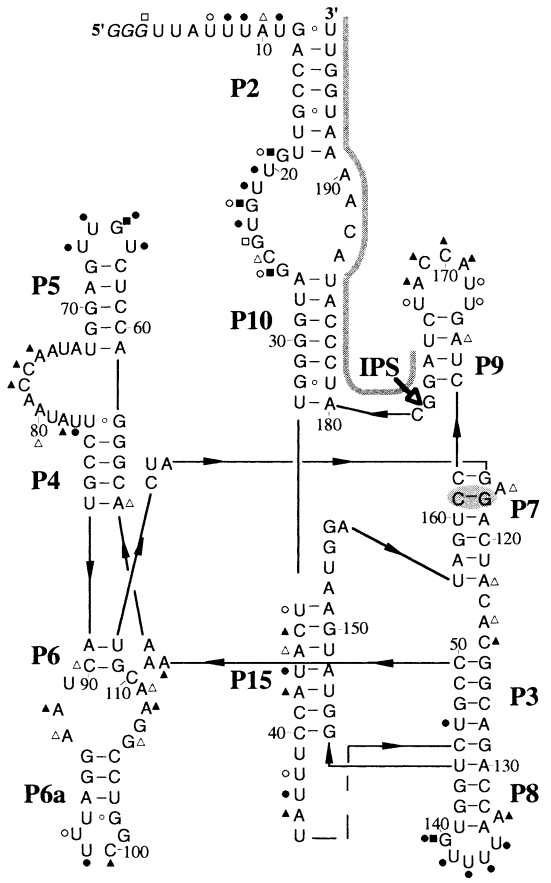

FIGURE 7: Sites of chemical modification superimposed on a revised secondary structure model of pre-NanGIR1. The various symbols indicate strong (▲) and weak (△) DMS modification, strong (●) and weak (○) CMCT modification, and strong (■) and weak (□) kethoxal modification. Determination of the degree of modification is based on PhosphorImager quantitation as described in Materials and Methods. Note that mapping of the 20 nucleotides 3′ to the IPS (gray, solid bar) was not possible due to hybridization of the reverse transcription primer to this site.

Chemical probing was performed in the presence of 25 mM $MgCl_2$ and 800 mM KCl, conditions under which pre-NanGIR1 is most reactive (see above). Modification was done at 25 °C rather than at 45 °C in order to minimize site-specific cleavage of the precursor. Chemical modification of NanGIR1 (product 1) RNA was carried out in parallel. The sites of modification were essentially identical with those of the precursor, suggesting that the secondary structure of the ribozyme does not undergo substantial change after cleavage, and showing that small amounts of product 1 present in the precursor modification reactions do not affect the chemical modification results. The sites of chemical modification are superimposed on a secondary structure model in Figure 7. The modified sites predominantly occur in proposed single-stranded regions, consistent with the model, with the exception of the P15 pseudoknot.

Mutational Analysis of the P15 Pseudoknot. Two possible structures for the P15 pseudoknot are shown in Figure 8. Model A, taken from Einvik and colleagues (*17*), is supported by comparative analysis of five *Naegleria* GIR1 RNAs, although the single compensatory base pair change does not constitute phylogenetic proof. In addition, this model appears to disagree with our chemical modification results, as heavily modified U34−A38 are base paired. By shifting the right-hand strand downward, a new base pairing possibility is achieved (model B) that is consistent with the

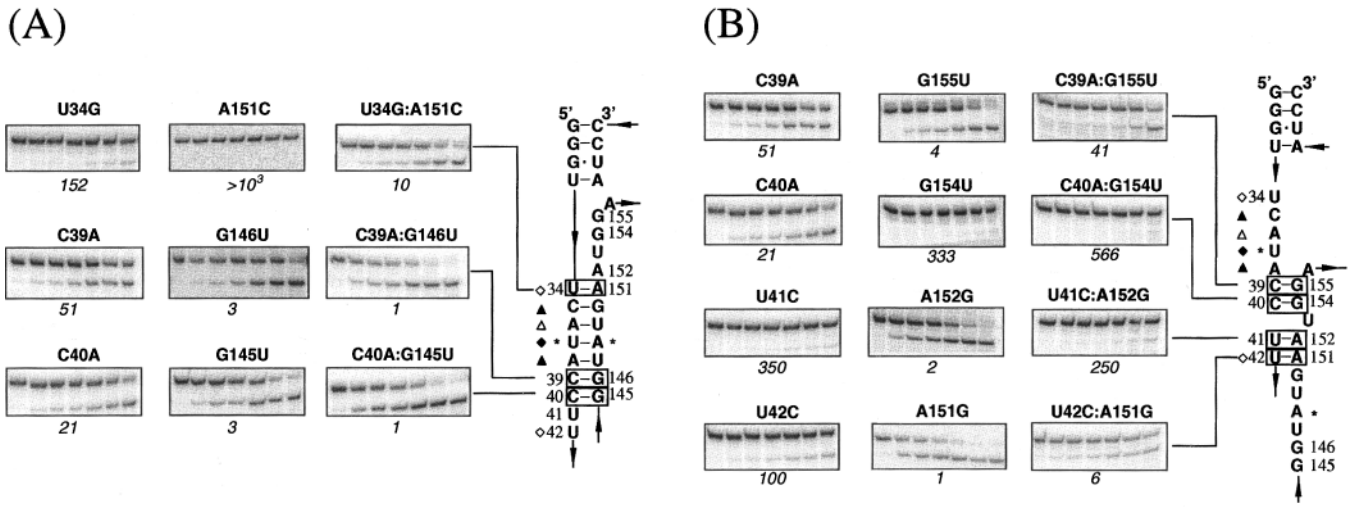

FIGURE 8: Site-directed mutagenesis of the P15 pseudoknot. Models for the P15 pseudoknot are based on (A) phylogenetic sequence comparison among five GIR1 RNAs from five species of *Naegleria* (*17*) and (B) the chemical modification results presented herein. The two models differ simply in the register of the two strands forming the P15 pseudoknot. For example, in both models, C39 and C40 are base paired, but to different partners (G146 and G145 in model A versus G155 and G154 in model B). Using site-directed mutagenesis, single mutations were introduced for nucleotides 32−42 and 145−155. The activity of each mutant was assayed as described in Materials and Methods, and the fold decrease in activity relative to that of the wild type was determined (numbers in italics). Where the single mutation resulted in a greater than 20-fold decrease in activity, a second mutation was introduced to test for rescue of activity. For clarity, not all mutations are shown. Asterisks identify the site of the single covariation seen by phylogenetic analysis.

chemical modification, but does not account for the single covariation seen by phylogenetic analysis (asterisks in Figure 8).

To test the structural models, this region of the RNA was analyzed by site-directed mutagenesis (Figure 8). Most single mutations on either strand of the proposed P15 pseudoknot resulted in 4−350-fold decreases in activity relative to that of wild-type pre-NanGIR1, suggesting that this region of the RNA is important for proper folding and/or catalytic viability of the RNA. Specifically, mutation of C39 or C40 resulted in a greater than 20-fold decrease in activity, which could be almost completely restored by compensatory mutations of G146 and G145, respectively (see model A). This restoration of activity was specific, as constructs with compensatory mutations G154U or G155U (model B) did not rescue. The double mutation C40A:G154U resulted in a 566-fold decrease in activity. These results show that C39 and C40 are base paired with G146 and G145, respectively, thereby supporting the bottom portion of the duplex in model A. Considering the chemical modification data, however, it was still not clear whether the top half of the proposed helix actually formed. Therefore, mutations in U34 and A151 were analyzed. Each single mutation almost eliminated activity, while the double mutation U34G:A151C restored activity to within 10-fold of that of the wild type. These results support the conformation of the P15 pseudoknot shown in model A (Figure 8A).

DISCUSSION

NanGIR1 Looks Like a Group I Intron. The structure of NanGIR1 was proposed to resemble that of a group I intron in that it contained paired elements P3−P10 and a putative G-binding site (*17*). We have used chemical modification studies to verify that pre-NanGIR1 has most of the elements conserved in group I introns (Figure 1A) (*4*). Specifically, NanGIR1 can be discussed in terms of three building blocks, P4−P5−P6, P2−P10−P15, and P8−P3−P7 (Figure 7). P7 contains a G-binding site judging by the presence of the G118·C161 base pair and the adjacent bulged A (*31*). Johansen and colleagues (*17*) have shown that mutation of G118 at the G-binding site abolishes hydrolysis activity, which suggests that, although this intron has lost some structural elements necessary for self-splicing, it has retained the ability to bind guanosine at the active site. Pre-NanGIR1 lacks the base-paired region P1 which in the self-splicing group I introns contains the internal guide sequence (IGS) for alignment of the 5′-exon (*32*, *33*). Since pre-NanGIR1 is involved in hydrolytic processing and not splicing, it does not require this structural element.

The IPS of pre-NanGIR1 resembles the 3′SS of other group I introns in that it contains a conserved guanosine nucleotide (G178) immediately preceding the processing site, and retains the P9 and P10 elements (Figure 7). In particular, the intron's secondary structure is much like that of the group I intron from *Pneumocystis carinii*, which has its 3′SS guanosine immediately after P9 (*34*). In the *Tetrahymena*, *Anabaena*, and *sunY* introns, the 3′-terminal guanosine must bind in the G-binding site for the second step of self-splicing (*6*, *7*, *35*, *36*). We hypothesize that G178 of NanGIR1 binds at the G-binding site, thereby positioning the IPS close to the nucleophile. In support of this proposal, mutation of G178 resulted in complete loss of activity, and argininamide, which blocks the binding of exogenous guanosine to the G site of other group I introns (*23*), also inhibited pre-NanGIR1 self-cleavage. As in other group I introns, we expect that the P9 and P10 elements help determine which guanosine will bind in the G-binding site (*15*). P10 of pre-NanGIR1 resembles that of the self-splicing introns in that the sequence 3′ of the IPS (or in *Tetrahymena*, 3′ of 3′SS) base pairs with a region close to the 5′-end of the intron. P10 is connected to P2 via an internal loop, and the half of it that we were able to monitor by chemical modification appears to be very accessible and unstructured.

Pre-NanGIR1 has two features unique to the GIR1 family of introns. First, P4 consists of five base pairs, as shown through chemical modification, instead of the canonical six

base pairs, and is connected to P5 via an 11-nucleotide bulge rather than by the more symmetric internal loop seen in other group I introns (Figure 7). Deletion of this bulge (A73−U83) results in a greater than 50-fold decrease in activity (data not shown), which suggests that this region of NanGIR1 is involved in tertiary interactions.

Second, pre-NanGIR1 contains a pseudoknot (P15) that is composed of the strand connecting P10 and P3, and the strand connecting P8 and P7 (Figures 7 and 8; *17*). We found that single mutations that disrupt base pairing within the pseudoknot decrease the activity of NanGIR1. However, the accessibility of the P15 pseudoknot to chemical modification suggests that this base-paired region may be dynamic. Recall that chemical modification of RNA probes the structure of the ground state of a molecule, whereas site-directed mutagenesis, in which the activity of the RNA is monitored, probes the structure of the transition state. Therefore, differences in models generated by the two methods may indicate a change in the conformation of that region of the RNA upon approach to the transition state. The results for pre-NanGIR1 suggest that the P15 pseudoknot could consist of four base pairs in its ground state, which may rearrange upon approach to the transition state into a seven-base pair pseudoknot (Figure 8). Another possibility is that this duplex is under strain so that the top half of P15 is continuously pairing and unpairing.

NanGIR1 Acts Like a Group I Intron. Pre-NanGIR1, like group I introns, can be thought to form a catalytic active site since mutations far from the internal processing site (e.g. within P15, and the P4/P5 bulge) significantly decrease activity. This intron catalyzes site-specific hydrolysis at the IPS, at a rate of ~0.03 min^{-1} at pH 7.5. The reaction is efficient in that ~95% of the molecules react under optimal conditions (Figure 3B). It is first-order in [OH^-] in the pH range of 5−8.5 (Figure 5B), similar to that seen for site-specific hydrolysis of the circular form of the *Tetrahymena* intron (*37*). This pH dependence reflects a requirement for hydroxide ion or for removal of a proton in the transition state for the rate-limiting step, which could be the chemical or a conformational step. An attractive model is that between pH 5 and 8.5, the observed rate reflects the chemical step of the reaction, the nucleophilic attack of OH^- (or Mg^{2+}-coordinated OH^-) directly on the phosphate bond at the IPS. The plateau in the rate seen at high pH could reflect a partial denaturation of the RNA due to deprotonation of uracil and guanine, nonspecific degradation by alkaline hydrolysis, or a change in the rate-limiting step.

The observed pH dependence justifies the calculation of a second-order rate constant for hydrolysis of the IPS phosphodiester bond. This reaction is fast relative to the nonspecific hydrolysis of RNA and 2 orders of magnitude faster than site-specific hydrolysis of the *Tetrahymena* intron at the circularization site, which follows the 3′-terminal G of the intron (Table 1). The latter observation is not surprising as the role of GIR1 is to specifically process the 5′-end of the mRNA for the endonuclease, whereas in the circular form of the *Tetrahymena* intron, the hydrolysis is considered simply a poor side reaction. Pre-NanGIR1 hydrolysis is 3 orders of magnitude slower than the reaction catalyzed by RNase P RNA, which must process pre-tRNAs with multiple turnover (Table 1).

Thermodynamic parameters of activation associated with the NanGIR1 hydrolysis show the mechanistic similarity between the hydrolysis reaction of pre-NanGIR1 and hydrolysis at the 3′SS of typical group I introns. Values of $\Delta H^{\ddagger}$ and $\Delta S^{\ddagger}$ for the hydrolysis reaction of the L-21 *Sca*I version of the *Tetrahymena* group I intron have previously been measured (*14*). Our values of ~26 kcal mol^{-1} K^{-1} for $\Delta H^{\ddagger}$ and near zero for $\Delta S^{\ddagger}$ are within error of these values.

Table 1: Rate Constants for Alkaline Hydrolysis of Phosphate Diesters[a]

compound	T (°C)[b]	k[c] (min^{-1} M^{-1})	ref
dimethyl phosphate[d]	25	2×10^{-10}	51
	42	2×10^{-9}	51
ethylene phosphate[d]	25	3×10^{-2}	51
RNA	27	2×10^{-2}	52
uridine cyclic 2′,3′-phosphate	30	3×10^{-1}	53
	40	5×10^{-1}	53
poly(A) + 0.2 mM Mg^{2+}	64	<1	54
Tetrahymena circularization site	42	2×10^{3}	37
pre-NanGIR1	**45**	$\mathbf{1 \times 10^{5}}$	**this work**
RNase P RNA	37	4×10^{8}	48 and 55

[a] Table reproduced and modified from ref 37. [b] Available rate constants determined at temperatures close to 45 °C are given. [c] $k = k_{obs}/[OH^-]$. [d] Corrected for fraction of hydrolysis via P−O bond cleavage (0.1) according to ref 56.

In the *Tetrahymena* group I intron, Mg^{2+} ions have been shown to participate in RNA folding, substrate binding, and catalysis (*38*, *39*). It is plausible that Mg^{2+} ions play similar roles in pre-NanGIR1. The presence of divalent metal ions (Mg^{2+} or Mn^{2+}) is essential for pre-NanGIR1 activity. The failure of Ca^{2+}, monovalent ions, or polyamines to substitute suggests that this cofactor is not simply a structural requirement, and that the divalent ion may participate directly in the hydrolysis reaction. Indeed, there is strong expectation of specific divalent cation stabilization of the oxyanion leaving group and destabilization of the ground state as found for group I intron splicing (*38*, *40*). In addition, the Mg^{2+} may coordinate the nucleophile (*41*). The requirement for Mg^{2+} of pre-NanGIR1 catalysis is not absolute, as Mn^{2+} can substitute at an even lower concentration (Figure 4A). Similar behavior was observed in the *Tetrahymena* group I intron where the rate of cleavage in the presence of $MnCl_2$ is faster than that with $MgCl_2$ (*41*, *42*). This behavior may be due to the relative pK_as of the aqua ions, $Mn(H_2O)_6^{2+}$ (10.0) and $Mg(H_2O)_6^{2+}$ (11.4) (*43*), since the hydroxide−metal ion complex will be 50-fold more prevalent at neutral pH when Mn^{2+} replaces Mg^{2+} as the cation. Thus, it does not necessarily reflect a preference by the RNA for binding one divalent ion over the other.

The requirement for 25 mM $MgCl_2$ might be necessary to compete with the high monovalent concentration required for proper folding or catalysis. *In vitro*, pre-NanGIR1 requires 1 M KCl for maximal reactivity (Figure 4B). *In vivo*, where high concentrations of salt are not available, pre-NanGIR1 may require a protein cofactor for efficient folding or catalysis. Several examples of a protein requirement being substituted by high concentrations of monovalents have been reported. In the fifth intron (bI5) of the gene encoding apocytochrome *b* in yeast mitochondria, the rate of splicing increased at high concentrations (1 M) of monovalent cation; the choice of monovalent also significantly affected the reaction. The monovalent cation is proposed to play a role similar to that of the protein component (CBP2) of bI5 in

that they titrate the local anionic repulsion within the RNA, and promote folding of the RNA into a catalytically active conformation (*44*). The P RNA component of RNase P is another system which requires high salt (usually 1 M NH_4^+) for activity (*45*). The protein component in RNase P plays a role in promoting the tight binding of P RNA to the pre-tRNA (*45*−*48*), and Beebe and colleagues (*48*) have shown that monovalent cations (NH_4^+, Cs^+, K^+, or Rb^+) carry out the same function. Although pre-NanGIR1 may require a protein for proper folding or catalysis, this component has not yet been identified.

As noted, monovalent ions have the potential to influence the structure of the RNA, but how a specific monovalent ion promotes the folding or unfolding of RNA is not well-understood. A well-studied example of how K^+ affects structure is the formation of a G quartet. This structure, a square planar, hydrogen-bonded array of four guanine bases, is stabilized by physiological concentrations of K^+ ions and, to a lesser extent by Na^+ ions. The ionic specificity is a result of the size of the ion binding site as well as the electronegativity of the carbonyl oxygens on the guanine base (*49*). Although an examination of the primary sequence of pre-NanGIR1 does not show any regions which we expect to form a G quartet, it is possible that such an interaction, or something similar, could form in the catalytically active structure. Pre-NanGIR1 prefers K^+ for folding, but Na^+ can substitute to a lesser degree. For K^+, both the ionic (1.52 Å) and hydrated (2.76 Å) radii are larger than those of Na^+ (1.16 and 2.32 Å, respectively). Therefore, the specificity could be related to the size of the cation binding site regardless of the hydration sphere. The inhibition by Li^+ could be due to its small ionic radius, which allows this monovalent to bring the phosphate backbone too close together, thereby destabilizing the RNA tertiary structure (*50*). Alternatively, hydrated Li^+ (3.50 Å), which is much larger than either hydrated K^+ or Na^+, may distort the monovalent binding site(s) and thereby affect the catalytic activity. A final possibility is that Li^+ (or hydrated Li^+) may compete with Mg^{2+} and thereby displace the catalytically required Mg^{2+} ion(s). In the absence of a tertiary structure, we cannot distinguish between the effects of ionic radius versus hydration radius on monovalent specificity, nor can we identify the monovalent binding site(s).

In summary, we have further defined the catalytic activity and the secondary structure of the catalytic element, NanGIR1, one of six natural examples of a novel class of introns whose sole function is site-specific hydrolysis at an IPS. NanGIR1 is a "stripped down" group I intron which has lost structural features unnecessary for site-specific hydrolysis at the 3′SS, and gained a novel pseudoknot. It has evolved to be a rather efficient catalytic element, catalyzing hydrolysis at a rate 2 orders of magnitude faster than that of the 3′SS cleavage of conventional group I introns. Additional kinetic as well as tertiary structure analysis of this and other GIR1 RNAs will further elucidate the mechanistic and structural features that account for their catalytic activity.

ACKNOWLEDGMENT

We thank Steinar Johansen for the generous gift of Nan-290 clone from which all clones for this work were derived, Steinar Johansen and Volker Vogt for sharing unpublished data on DirGIR1 RNA and for numerous discussions, Cheryl Grosshans and Elaine Podell for synthesis of DNA oligomers, Anne Gooding for the kinetic analysis of the 11-nucleotide bulge (between P4 and P5) deletion mutant, and members of the Cech and Uhlenbeck labs for critical reading of the manuscript and helpful discussions.

REFERENCES

1. Belfort, M. (1991) *Cell 64*, 9−11.
2. Lisacek, F., Diaz, Y., and Michel, F., (1994) *J. Mol. Biol. 235*, 1206−1217.
3. Yamada, T., Tamura, K., Aimi, T., and Songsri, P. (1994) *Nucleic Acids Res. 22*, 2532−2537.
4. Cech, T. (1993) in *The RNA World* (Gesteland, R. F., and Atkins, J. F., Eds.) pp 239−269, Cold Spring Harbor Laboratory Press, Plainview, NY.
5. Guo, Q., and Lambowitz, A. M. (1992) *Genes Dev. 6*, 1357−1372.
6. Michel, F., Hanna, M., Green, R., Bartel, D. P., and Szostak, J. W. (1989) *Nature 342*, 391−395.
7. Been, M. D., and Perrotta, A. T. (1991) *Science 252*, 434−437.
8. Zaug, A. J., and Cech, T. R. (1986) *Science 231*, 470−475.
9. Kay, P. S., and Inoue, T. (1987) *Nature 327*, 343−346.
10. Rocheleau, G. A., and Woodson, S. A. (1994) *Nucleic Acids Res. 22*, 4315−4320.
11. Inoue, T., Sullivan, F. X., and Cech, T. R. (1986) *J. Mol. Biol. 189*, 143−165.
12. Salvo, J. L. G., Coetzee, T., and Belfort, M. (1990) *J. Mol. Biol. 211*, 537−549.
13. Williams, K. P., Fujimoto, D. N., and Inoue, T. (1994) *J. Biochem. (Tokyo) 115*, 126−130.
14. Legault, P., Herschlang, D., Celander, D. W., and Cech, T. R. (1992) *Nucleic Acids Res. 20*, 6613−6619.
15. Van Der Horst, G., and Inoue, T. (1993) *J. Mol. Biol. 229*, 685−694.
16. Decatur, W. A., Einvik, C., Johansen, S., and Vogt, V. M. (1995) *EMBO J. 14*, 4558−4568.
17. Einvik, C., Decatur, W. A., Embley, T. M., Vogt, V. M., and Johansen, S. (1997) *RNA 3*, 710−720.
18. Johansen, S., and Vogt, V. M. (1994) *Cell 76*, 725−734.
19. Johansen, S., Embley, T. M., and Willassen, N. P. (1993) *Nucleic Acids Res. 21*, 4405.
20. Zaug, A. J., Lingner, J., and Cech, T. R. (1996) *Nucleic Acids Res. 24*, 532−533.
21. Donis-Keller, H., Maxam, A. M., and Gilbert, W. (1977) *Nucleic Acids Res. 4*, 2527−2538.
22. Zaug, A. J., and Cech, T. R. (1995) *RNA 1*, 363−374.
23. Yarus, M. (1989) *Biochemistry 28*, 980−988.
24. Wu, H.-N., and Lai, M. C. C. (1990) *Mol. Cell Biol. 10*, 5575−5579.
25. Forster, A. C., and Symons, R. H. (1987) *Cell 49*, 211−220.
26. Van Der Horst, G., Christian, A., and Inoue, T. (1991) *Proc. Natl. Acad. Sci. U.S.A. 88*, 184−188.
27. Hanna, M., and Szostak, J. W. (1994) *Nucleic Acids Res. 22*, 5326−5331.
28. Tanner, M. A., and Cech, T. R. (1996) *RNA 2*, 74−83.
29. Inoue, T., and Cech, T. R. (1985) *Proc. Natl. Acad. Sci. U.S.A. 82*, 648−652.
30. Stern, S., Wilson, R. C., and Noller, H. F. (1986) *J. Mol. Biol. 192*, 101−110.
31. Michel, F., and Westhof, E. (1990) *J. Mol. Biol. 216*, 585−610.
32. Davies, R. W., Waring, R. B., Ray, J. A., Brown, T. A., and Scazzocchio, C. (1982) *Nature 300*, 719−724.
33. Cech, T. R., and Herschlag, D. (1996) in *Nucleic Acids and Molecular Biology: Catalytic RNA* (Eckstein, F., and Lilley, D. M. J., Eds.) pp 1−17, Springer-Verlag, New York.
34. Leibowitz, M. J., and Liu, Y. (1993) *Nucleic Acids Res. 21*, 2415−2421.
35. Golden, B. L., and Cech, T. R. (1996) *Biochemistry 35*, 3649−3874.
36. Michel, F., Netter, P., Xu, M.-Q., and Shub, D. (1990) *Genes Dev. 4*, 777−788.

37. Zaug, A. J., Kent, J. R., and Cech, T. R. (1985) *Biochemistry 24*, 6211−6218.
38. Piccirilli, J. A., Vyle, J. S., Caruthers, M. H., and Cech, T. R. (1993) *Nature 361*, 85−88.
39. McConnell, T. S., Herschlag, D., and Cech, T. R. (1997) *Biochemistry 36*, 8293−8303.
40. Narlikar, G. J., Gopalakrishnan, V., McConnell, T. S., Usman, N., and Herschlag, D. (1995) *Proc. Natl. Acad. Sci. U.S.A. 92*, 3668−3672.
41. Weinstein, L. B., Jones, B. C. N. M., Cosstick, R., and Cech, T. R. (1997) *Nature 388*, 805−808.
42. Grosshans, C. A., and Cech, T. R. (1989) *Biochemistry 28*, 6888−6894.
43. Huheey, J. E. (1983) in *Inorganic Chemistry-Principles of Structure and Reactivity*, p 295, Harper & Row, New York.
44. Partono, S., and Lewin, A. S. (1991) *Nucleic Acids Res. 19*, 605−610.
45. Reich, C., Olsen, G. J., Pace, B., and Pace, N. R. (1988) *Science 239*, 178−181.
46. Gardiner, K. J., Marsh, T. L., and Pace, N. R. (1985) *J. Biol. Chem. 260*, 5415−5419.
47. Pan, T. (1995) *Biochemistry 34*, 902−909.
48. Beebe, J. A., Kurz, J. C., and Fierke, C. A. (1996) *Biochemistry 35*, 10493−10505.
49. Williamson, J. R., Raghuraman, M. K., and Cech, T. R. (1989) *Cell 59*, 871−880.
50. Knitt, D. S., and Herschlag, D. (1996) *Biochemistry 35*, 1560−1570.
51. Kumamoto, J., Cox, J. R., and Westheimer, F. H. (1956) *J. Am. Chem. Soc. 78*, 4858−4860.
52. Bock, R. M. (1967) *Methods Enzymol. 12A*, 218−221.
53. Abrash, H. I., Cheung, C.-C. S., and Davis, J. C. (1967) *Biochemistry 6*, 1298−1303.
54. Butzow, J. J., and Eichhorn, G. L. (1965) *Biopolymers 3*, 95−107.
55. Smith, D., and Pace, N. (1993) *Biochemistry 32*, 5273−5281.
56. Haake, P. C., and Westheimer, F. H. (1961) *J. Am. Chem. Soc. 83*, 1102−1109.
57. Cech, T. R., Damberger, S. H., and Gutell, R. R. (1994) *Nat. Struct. Biol. 1*, 273−280.

BI9718595